Sustainable Energy & Fuels

Ethanol as a Hydrogen Carrier with a Value-Added Co-Product

Journal:	*Sustainable Energy & Fuels*
Manuscript ID	SE-COM-10-2024-001524
Article Type:	Communication
Date Submitted by the Author:	31-Oct-2024

Complete List of Authors:	Rander, Andrew; University of Southern California, Loker Hydrocarbon Research Institute Kohl, Shayna; University of Southern California, Loker Hydrocarbon Research Institute Cherepakhin, Valeriy; University of Southern California, Loker Hydrocarbon Research Institute Do, Van; University of Southern California, Loker Hydrocarbon Research Institute Zhang, Long; University of Southern California, Loker Hydrocarbon Research Institute Breunig, Hanna; Lawrence Berkeley National Laboratory, Williams, Travis; University of Southern California, Loker Hydrocarbon Research Institute

COMMUNICATION

Ethanol as a Hydrogen Carrier with a Value-Added Co-Product

Andrew R. Rander,[a] Shayna R. Kohl,[a] Valeriy Cherepakhin,[a] Long Zhang,[a] Van K. Do,[a] Hanna Breunig,[b] and Travis J. Williams*[a]

Received 00th January 20xx,
Accepted 00th January 20xx

DOI: 10.1039/x0xx00000x

Traditional liquid organic hydrogen carriers (LOHCs) rely on return/re-charge of the carrier and financial subsidy, we show here that ethanol, available at scale from fermentation, can be a revenue-positive hydrogen carrier, owing to the value of its potassium acetate co-product, itself an emerging fertilizer.

High efficiency liquid organic hydrogen carriers (LOHCs) are an essential link in H_2 storage, because they enable storage densities superior to the parent compressed gas and are easy to transport. Traditionally, the spent fuel that results from H_2 release from a 2-way carrier is then transported to a source of low-cost hydrogen for re-charge. Commercialization of this concept has seen the use of functionalized toluenes; however, these only operate with financial subsides.[1] While ethanol to ethyl acetate has been demonstrated as a 2-way hydrogen carrier that releases one equivalent of H_2 per ethanol,[2] we reexamine ethanol here, contemplating a 1-way carrier strategy that produces two equivalents of H_2 and potassium acetate, an advantageous, emerging fertilizer.

Potassium acetate, a high value agrochemical, has emerged as a superior source of potassium for plants, with a market projected to reach $290.66 million by the end of 2030.[3,4] Thus, we see ethanol as a 1-way H_2 carrier that is "self-subsidizing" by the value created in its dehydrogenated co-product; in fact at present pricing the value increase is ca. 4x. Incumbent technologies for potassium acetate manufacturing involve multi-step syntheses, including the Monsanto or Cativa process, relying on a homogeneous rhodium or iridium catalysts respectively to affect the carbonylation of methanol derived from petrochemical sources.[5]

While a direct catalytic ethanol-to-acetate process is a straightforward extension of known alcohol-to-carboxylate dehydrogenation methods,[6–13] such reactions typically require a high boiling co-solvent and pressurized systems have never been developed. Further, process commercialization would also require scalable, high turnover, solvent-free conditions and a pressure tolerant catalytic system enabling separation of H_2 gas and solid KOAc; technology which has not been introduced. Selectivity also frustrates alcohol dehydrogenation catalysts: while several examples of catalytic ethanol dehydrogenation form the Tishchenko product, ethyl acetate, or the Guerbet product, 1-butanol; none focus on the dehydrogenation subsidizing the production of hydrogen with the carboxylate.[2,9,13–21] We, therefore, see a need to introduce dehydrogenation of ethanol to potassium acetate with the ability to self-pressurize the produced hydrogen for on-demand hydrogen production.

Based on our group's work with iridium chelates for the dehydrogenation of formic acid,[22–24] we screened complex **1** (Figure 1) at 0.01 mol% in neat ethanol with an excess of potassium hydroxide. ^{1}H NMR confirms acetate production after a 24-hour reaction. Complex **1** (CCDC 1415049) and its ruthenium congener (**3**; CCDC 1510912)[25] both perform modestly with the acetate yields of 24% and 40%, respectively (Table 1, entries 1 and 2). NMR suggests that **3** has greater selectivity than **1**, as the latter contained Guerbet products such as 2-ethyl-1-butanol while the former contains only product and trace butyrate (see ESI).

We screened a group of compounds (Figure 1) as catalysts in the ethanol dehydrogenation (Table 1). The reaction was conducted between ethanol and KOH·½H_2O (1:1) in boiling toluene for 42 h with 0.1 mol% catalyst. ^{1}H NMR analysis of the products consistently shows acetate (1.90 ppm), formate (8.56 ppm), and butyrate ions (2.13 ppm). Quantitative ^{1}H NMR (vs. internal DMF standard) and acid-base back titration provide the molar distribution of the carboxylates and the conversion of KOH. Several complexes (entries 1–4, 6–9, 13–17) performed poorly generating less than 40%.[22,25–31] Complexes **2**–**3**, **16**–**17**, and **19** produced large portions of formate, apparently generated by decarbonylation of an intermediate acetaldehyde; ruthenium(II) complex **16** prefers this pathway (8:1, formate to acetate).[25–27] The complexes that afforded the highest yields of acetate are ruthenium-based (entries 5,

[a] Donald P. and Katherine B. Loker Hydrocarbon Research Institute, Wrigley Institute for Environment and Sustainability, and Department of Chemistry, University of Southern California, Los Angeles, California, 90089-1661, USA
[b] Sustainable Energy Systems Group, Energy Analysis and Environmental Impacts Division Lawrence Berkeley National Lab, 1 Cyclotron Road, 90-2012 Berkeley, California, 94720, USA

Electronic Supplementary Information (ESI) available: Experimental procedures and characterization data (PDF). See DOI: 10.1039/x0xx00000x

10–12, 70–90%).[21,32,33] For example, we designed **5** based on the known efficiency of NHC-ligated iridium dehydrogenation catalysts, which maintain both good reactivity for H_2 abstraction while remaining resistant to deactivation.[34]

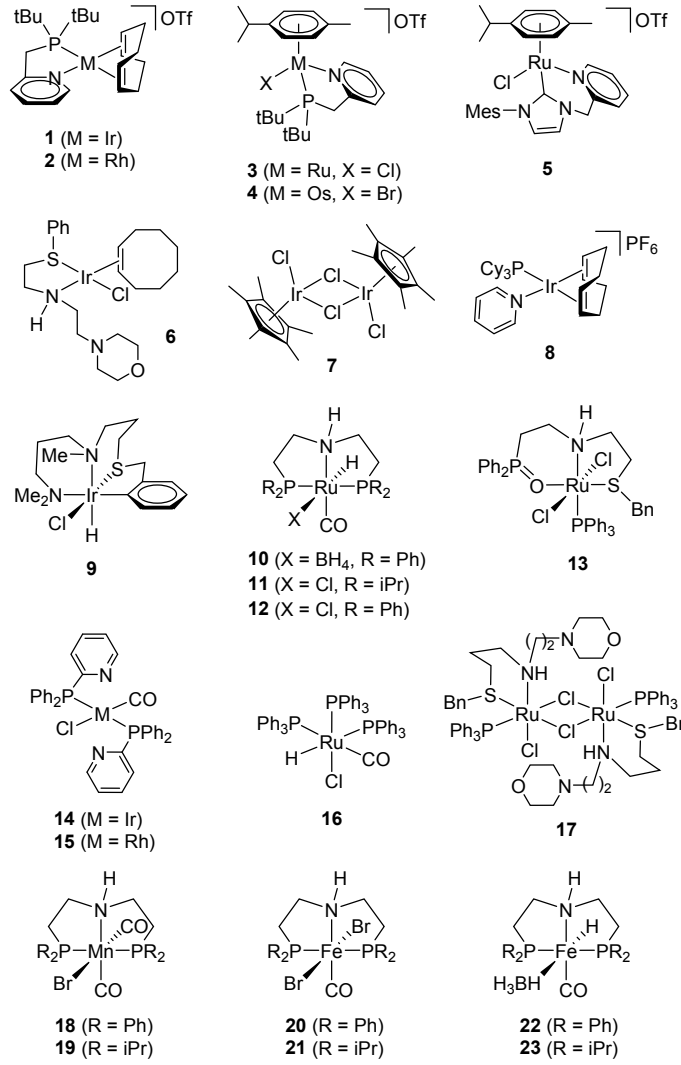

Figure 1: Compounds tested as ethanol dehydrogenation catalysts.

Pincer complexes **10**–**12** show promising reactivity (entries 10–12); we attribute the advantage of **10** over **12** to the known lability of the borohydride ligand to facilitate catalyst initiation.[21,31,32] Finally, we measured the performance of **10** and a series of manganese(I) and iron(II) PNP-pincer complexes **18**–**23** (entries 18-23), which are known to catalyze alcohol dehydrogenation and hydrogen borrowing reactions.[35–40] Despite being derived from the earth-abundant metals, complexes **18**–**23** show inferior activity (TOF = (1–5)×10^{-3} s^{-1})compared to their ruthenium congener **10** (TOF = 1.3 s^{-1}). [35–40] Unlike **10**, these also suffer from photosensitivity (**19**) and hydrolysis (**21**) making them unfit for the practical use.[20,40] Of all of the catalysts we screened, **23** returned the highest portion of butyrate, apparently through a Guerbet pathway. We had previously suggested that the ruthenium metal center is of upmost importance in catalytic dehydrogenation efficiency which is consistent with our findings.[7,20]

We selected catalyst **10** to proceed to optimize conditions (Table 2) due to its rate and selectivity. We found that reducing the KOH loading to 0.5 eq or less suppresses the side processes and increases the acetate yield to 99% (entries 5 and 6). Furthermore, we showed that a high yield of acetate (96%) is attainable in neat ethanol at 80 °C (entry 7). By contrast, we observe (^{1}H NMR) that operating the reaction in excess base lowers yields and compromises purity. These observations point to an operational scenario of slow addition of ethanol/hydroxide solution in a continuous process.

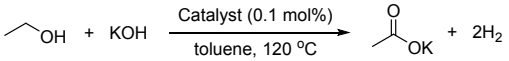

Table 1: Catalyst screening[a]

Entry	Catalyst	Acetate (%) [b]	Anions (mol%) [c]			
			OH^-	Formate	Acetate	Butyrate
1	1	10	76	2	22	0
2	2	29	63	22	15	0
3	3	26	60	12	27	1
4	4	37	71	0	28	< 1
5	5	87	18	3	79	0
6	6	18	58	1	40	< 1
7	7	7	80	1	19	0
8	8	19	71	1	28	0
9	9	1	63	2	35	0
10	10	80	5	3	90	1
11	11	75	21	7	71	1
12	12	68	14	3	83	0
13	13	14	66	0	32	2
14	14	17	73	1	26	0
15	15	12	87	1	11	< 1
16	16	7	64	32	4	0
17	17	24	56	25	19	0
18	18	26.5	51	< 1	49	< 1
19	19	7	61	4	39	2
20	20	66	52	2	47	< 1
21	21	8	70	4	30	< 1
22	22	15	83	3	20	< 1
23	23	9	69	3	31	5

[a]Conditions: catalyst, KOH·½H_2O (0.56 g, 9 mmol), ethanol (0.92 g, 20 mmol), and toluene (10 mL) were heated at reflux (oil bath, 120 °C) under N_2 for 42 h. [b]Determined by ^{1}H NMR using DMF as an internal standard. [c]Determined by acid-base back titration and ^{1}H NMR.

Gas compression costs can contribute to 80% of hydrogen delivery costs,[41] depending on the application, and the entropy of dehydrogenation can supply this pressure cost-free.[23] We thus investigated self-pressurizing conditions for our reaction. While complex **10** delivers a modestly lower yield of (74%) when run under self-pressurizing conditions (Table 3, entry 4), complex **1** demonstrates improved performance under self-pressurizing conditions, achieving 67% yield (entry 1) compared to 24% yield under ambient conditions.

We've previously shown that **1** activates to a multi-metal cluster via carbonylation, which is facilitated by

pressurization.[23] Similar trends appear when varying the ratio of reactants at pressure as seen under ambient conditions (entries 4 and 5): decreasing the concentration of hydroxide resulted in 98% yield of acetate in a reaction of **10**. Further, conditions with six equivalents of ethanol to hydroxide resulted in 98% yield, demonstrating that co-solvent is unnecessary. With high yielding conditions, we turned to determine the efficiency of selected catalysts at increased scale (see ESI). Over the course of several months, **10** and **1** were each allowed to react on a 10-gram (KOAc) scale under our optimized ambient pressure, batch reaction conditions.

Table 2: Ethanol dehydrogenation with catalyst **10** under 1 atm[a]

Entry	KOH (eq.)	**10** (mol% vs. EtOH)	Carboxylates (mol%)[b]	Acetate (%)[c]
1	1.97	0.13	48	27
2	1.32	0.09	47	18
3	0.95	0.10	95	77
4	0.74	0.10	98	73
5	0.49	0.10	99	94
6[d]	0.14	0.02	96	87

[a]Conditions: **10**, KOH·½H_2O, ethanol (0.92 g, 20 mmol), and toluene (10 mL) were heated at reflux (oil bath, 120 °C) under N_2 for 42 h. [b]Determined by acid-base back titration. [c]Determined by ^{1}H NMR. [d]Conditions: **10**, KOH·½H_2O, and ethanol (5.53 g, 120 mmol) were heated at reflux (80 °C) under N_2 for 42 h.

Through three reactions using the same catalytic mixture, **10** showed 55,000 turnovers without loss of reactivity (See ESI Table S4). **1** delivered 168,000 turnover numbers over one three-month reaction, similarly without deactivation (See ESI Table S5). Catalyst **10** and **1** can be recovered and reused through several directed cycles presaging the use of a continuous operation reactor.

The mechanism of alcohol dehydrogenation with ruthenium Noyori type catalysts is well known.[21,42–48] System **10** appears to conform: the deprotonation of NH and dissociation of BH_4^- give the active catalyst **10a** (Scheme 1).[41, 42,44–46]Analysis of the post-catalytic mixture suggests the presence of two complexes **10b** and **10c** (89% yield combined).[49] These are *fac*- and *mer*-[(PNP)RuH_2(CO)] featuring hydride signals at δ_H = −6.64 ppm (**10b**), and −5.77, −5.88 ppm (**10c**). The ^{31}P{^{1}H} NMR contains signals at δ_P = 70.11 ppm (**10c**) and 60.45 ppm (**10b**) with no shared correlations in the ^{1}H-^{31}P HMBC.

Table 3: Ethanol dehydrogenation under self-pressurizing conditions[a]

Entry	Catalyst	EtOH (eq.)	Time (h)	Final pressure (bar)	Carboxylates (mol%)[b]	Acetate (%)[c]
1	1	1	45	8	67	64
2	1	2	25	6	50	28
3	5	1	47	9	66	70
4	10	1	45	9	74	82
5	10	2	45	14	98	95
6[d]	10	6	68	26	98	>99

[a]Conditions: catalyst (0.1 mol% vs. ethanol), KOH·½H_2O (1.92 g, 29.5 mmol), ethanol, and toluene (10 mL) were heated in a 125 mL Parr reactor at 120 °C. [b]Determined by acid-base back titration. [c]Determined by ^{1}H NMR. [d]Conditions: **10** (13 mg, 0.04 mol% vs. KOH), KOH·½H_2O (3.7 g), and ethanol (16 g) were heated in the Parr reactor at 120 °C.

Both compounds have the identical mass (*m/z* = 572 Da, MALDI)[50] and elemental composition. A ^{1}H{^{31}P} experiment (see ESI) shows interconversion between **10c** and **10b**, appropriate for respective *mer*- and *fac*- isomers. Complexes **10b** and **10c** are both active in the ethanol dehydrogenation. Interestingly, **10b** and **10c** are not stable to chlorinated solvents: a known dichloro derivative **10d** (δ_P = 48 ppm)[49] is formed within a few days in dichloromethane. Heating the reaction mixture past ethanol consumption results in further derivatization of **10b** and **10c**. MALDI suggests formation of a previously characterized diruthenium complex **10e** (*m/z* = 1141.63 Da).[45] Its formation can be seen as a base-induced tautomerization of **10a**, followed by insertion of Ru(0) to one of the phenyl-phosphorus bonds.

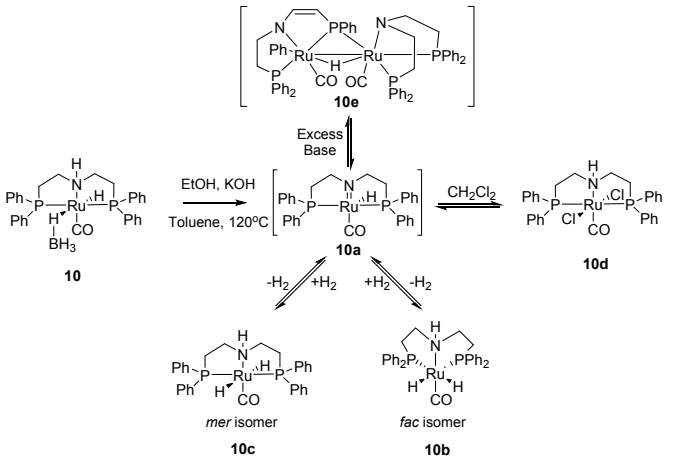

Scheme 1: Derivatization of **10** under the ethanol dehydrogenation conditions.

While some estimate negative carbon impact of ethanol as a gasoline additive, we calculate positive carbon impact in its use as a hydrogen carrier. Steam methane reforming (SMR) for H_2 production generates 11.9 kgCO_2-eq/kg-H_2. As corn or soybean production for ethanol or glycerol (via biodiesel), respectively, requires fertilizer and energy for conversion, the hydrogen generated from these carriers will have a carbon intensity. If 2 equivalents of H_2 are liberated, and the carbon intensity of manufacturing ethanol is 51.4 gCO_2-eq/MJ, the minimum carbon intensity of H_2 would be 8.03 kg-CO_2/kgH_2 without the production of co-products. The process emits biogenic CO_2 along with H_2, which in our case would eventually be emitted upon the use of the acetate co-product. Allocation of emissions between H_2 and coproducts can be done based on mass, energy content, or economic value: with a 1 to 41 weight ratio of H_2 to sodium acetate, mass allocation would result in a carbon intensity of 0.09 kgCO_2/kgH_2. For perspective, wind-powered electrolysis has a carbon intensity of 0.6 kgCO_2/kgH_2 assuming an electricity emission intensity of 11 g/kWh.[51]

The power of our reaction is the ability to produce pure H_2 with a coproduct whose value can negate production costs. The vast majority of hydrogen sold today is produced from non-renewable, hydrocarbon streams with only 4% of global hydrogen being considered “green hydrogen” typically

produced by electrolysing water, which still faces challenges of gas separation, selectivity, and metal cost.[52] Furthermore, the largest electrolysis units are owned and operated by the agrochemical industry,[52] a sector with a need for pure hydrogen and an efficient fertilizer production. While our method addresses both, its H_2 product is not "green" according to the electrolysis-based definition. Hydrogen derived from biomass is not classified in the current colour definition, so we refer to ours as "clear" hydrogen, submitting this as a suitable designation for hydrogen derived from biomass.

In sum, we have demonstrated the first direct one-pot synthesis of potassium acetate from neat ethanol, providing two equivalents of H_2, potentially at pressure, and a biologically advantageous fertilizer. The strategy obviates co-products, CO and CO_2, associated with formic acid and methanol dehydrogenation, [53–57] and eliminates nearly 99% of the carbon intensity of ethanol-based H_2 available for other methods. Several catalysts are effective for the reaction, with each offering useful features for use cases requiring pressure, longevity, or both. Popular Ru-MACHO systems are particularly attractive, and we show their speciation under ethanol dehydrogenation conditions. Overall, favorable carbon impact, yield, and selectivity of the system makes ethanol a very attractive 1-way liquid hydrogen carrier.

Author Contributions

Conceptualization, data curation, formal analysis, investigation, methodology, project administration, validation, visualization: A.R.R, S.R.K., V.C. Original Draft: A.R.R Synthesis of **5**: L.Z. Synthesis and crystal structure of **2**: V.D. Life-cycle analysis: H.B. Funding acquisition, resources, supervision, writing review & editing: T.J.W

Conflicts of interest

T.J.W is a founder of the Catapower Inc., which sells some complexes discussed herein.

Data availability

All data supporting this communication has been included and is available as part of the Supplemental Information.

- Crystallographic, Spectral, and Experimental Information (PDF)
- X-ray Data for **2** (CIF)
- X-ray Data for 5 (CIF)

Acknowledgements

This work is sponsored by the US Department of Energy, DE-EE0011096 (USC) and DE-AC02-05CH11231 (LBNL). A.R.R. thanks the Wrigley Institute for Environment and Sustainability for fellowship assistance. We thank the NSF (CHE-2018740, DBI-0821671, CHE-0840366), the NIH (S10 RR25432), and USC Research and Innovation Instrumentation Awards for analytical tools. We thank Mr. Justin Lim and Mr. Anushan Alagaratnam for insightful discussions.

Notes and references

1 A Final Link in the Global Hydrogen Supply Chain.
2 B. L. Tran, S. I. Johnson, K. P. Brooks, S. T. Autrey, *ACS Sustainable Chem. Eng.*, 2021, **9**(20), 7130.
3 W. E. Shafer, D. W. Reed., *Journal of Plant Nutrition*, 1986, **9**(2), 143–57.
4 Potassium Acetate Market Size 2023-2030 Global Industrial Analysis, Market Share, Top Key Players, https://www.linkedin.com/pulse/potassium-acetate-market-size-2023-2030-global-analysis-aiwale-ixipf/?trk=article-ssr-frontend-pulse_more-articles_related-content-card, (accessed March 2024).
5 A. W. Budiman, J. S. Nam, J. H. Park, R. I. Mukti, T. S. Chang, J. W. Bae, et al., *Catal. Surv. Asia.*, 2016, 20(3), 173–93.
6 V. Cherepakhin, T. J. Williams, *ACS Catal.*, 2018, 8(5), 3754–63.
7 V. Cherepakhin, T. J. Williams, *Synthesis*, 2021, 53(6),1023–34.
8 E. Balaraman, E. Khaskin, G. Leitus, D. Milstein, *Nature Chem.*, 2013, 5(2), 122–5.
9 A. Sarbajna, I. Dutta, P. Daw, S. Dinda, S. M. W. Rahaman, A. Sarkar, et al. *ACS Catal.*, 2017, 7(4), 2786–90.
10 D. R. Pradhan, S. Pattanaik, J. Kishore, C. Gunanathan, *Org. Lett.*, 2020, 22(5), 1852–7.
11 L. Zhang, D. H. Nguyen, G. Raffa, X. Trivelli, F. Capet, S. Desset, et al., *ChemSusChem.*, 2016, 9(12), 1413–23.
12 H. Li, M.B. Hall, *J Am Chem Soc.*, 2014, 136(1), 383–95
13 P. Sponholz, D. Mellmann, C. Cordes, P. G. Alsabeh, B. Li, Y. Li, et al., *ChemSusChem.*, 2014, 7(9), 2419–22.
14 M. Nielsen, H. Junge, A. Kammer, M. Beller, *Angewandte Chemie International Edition*, 2012, 51(23), 5711–3.
15 J. Zhang, G. Leitus, Y. Ben-David, D. Milstein, *J. Am. Chem. Soc.*, 2005, 127(31), 10840–1.
16 D. G. Gusev, *ACS Catal.*, 2016, 6(10), 6967–81.
17 H. Aitchison, R. L. Wingad, D. F. Wass, *ACS Catal.*, 2016, 6(10), 7125-7132.
18 N.V. Kulkarni, W. W. Brennessel, W. D. Jones, *ACS Catal.*, 2018, 8(2), 997–1002.
19 S. Chakraborty, P. E. Piszel, C. E. Hayes, R. T. Baker, W. D. Jones, *J. Am. Chem. Soc.*, 2015, 137(45), 14264–7.
20 D. H. Nguyen, Y. Morin, L. Zhang, X. Trivelli, F. Capet, S. Paul, et al., *ChemCatChem.*, 2017, 9(14), 2652–60.
21 M. Bertoli, A. Choualeb, A. J. Lough, B. Moore, D. Spasyuk, D. G. Gusev, *Organometallics*, 2011, 30(13), 3479–82.
22 J. J. A. Celaje, Z. Lu, E. A. Kedzie, N. J. Terrile, N. J. Lo, T. J. Williams, *Nat. Commun.*, 2016, 7(1), 11308.
23 V. K. Do, N. A. Vargas, A. J. Chavez, L. Zhang, V. Cherepakhin, Z. Lu, et al., *Catal. Sci. Technol.*, 2022, 12(23), 7182–9.
24 P. J. Lauridsen, Z. Lu, J. J. A. Celaje, E. A. Kedzie, T. J. Williams, *Dalton Trans.*, 2018, 47(38), 13559–64.
25 J. J. A. Celaje, X. Zhang, F. Zhang, L. Kam, J. R. Herron, T. J. Williams, *ACS Catal.*, 2017, 7(2), 1136–42.
26 P. A. Dub, B. L. Scott, J. C. Gordon, *Organometallics*, 2015, 34(18), 4464–79.
27 P. A. Dub, J. C. Gordon, Polydentate Ligands and Their Complexes for Molecular Catalysis. WO2015191505A1, 2015.
28 R. H. Crabtree, H. Felkin, G. E. Morris, *Journal of Organometallic Chemistry*, 1977, 141(2), 205–15.
29 P.A Dub, R. J. Batrice, J.C. Gordon, B.L. Scott, Y. Minko, J.G. Schmidt. R.F. Williams, *Org. Process Res. Dev.*, 2020, 24(3), 415-442.

30 G. Franciò, R. Scopelliti, C. G. Arena, G. Bruno, D. Drommi, F. Faraone, *Organometallics*, 1998, 17(3), 338–47.
31 . P. Farr, M. M. Olmstead, C. H. Hunt, A. L. Balch, *Inorg. Chem.*, 1981, 20(4), 1182–7.
32 W. Kuriyama, T. Matsumoto, O. Ogata, Y. Ino, K. Aoki, S. Tanaka, et al., *Org. Process Res. Dev.*, 2012, 16(1), 166–71.
33 W. Kuriyama, T. Matsumoto, Y. Ino, O. Ogata, Novel Ruthenium Carbonyl Complex Having a Tridentate Ligand and Manufacturing Method and Usage Therefor. WO2011048727A1, 2011.
34 L. S. Sharninghausen, R. H. Crabtree, *Israel Journal of Chemistry*, 2017, 57(10–11), 937–44.
35 J. C. Borghs, Y. Lebedev, M. Rueping, O. El-Sepelgy, *Org Lett.*, 2019, 21(1), 70–4.
36 S. Elangovan, C. Topf, S. Fischer, H. Jiao, A. Spannenberg, W. Baumann, R. Ludwig, K. Junge, M. Beller, *J. Am. Chem. Soc.*, 2016, 138(28), 8809-8814.
37 W. Ma, S. Cui, H. Sun, W. Tang, D. Xue, C. Li , et al., *Chemistry – A European Journal*, 2018, 24(50), 13118–23.
38 S. Chakraborty, H. Dai, P. Bhattacharya, N. T. Fairweather, M. S. Gibson, J. A. Krause, et al., *J. Am. Chem. Soc.*, 2014, 136(22),7869–72.
39 F. Schneck, M. Assmann, M. Balmer, K. Harms, R. Langer, *Organometallics*, 2016, 35(11), 1931-1943.
40 M. Andérez-Fernández, L. K. Vogt, S. Fischer, W. Zhou, H. Jiao, M. Garbe, S. Elangovan, K. Junge, H. Junge, R. Ludwig, M. Beller, *Angewandte Chemie International Edition*, 2017, **56**(2), 559–562.
41 Office of Fossil Energy. Hydrogen Strategy Enabling A Low-Carbon Economy, chrome-extension://efaidnbmnnnibpcajpcglclefindmkaj/https://www.energy.gov/sites/prod/files/2020/07/f76/USDOE_FE_Hydrogen_Strategy_July2020.pdf, (accessed March 2023).
42 P. A. Dub, J. C. Gordon, *Nat. Rev. Chem.*, 2018, 2(12), 396–408.
43 E. Alberico, A. J. J. Lennox, L. K. Vogt, H. Jiao, W. Baumann, H. J. Drexler, et al., *J. Am. Chem. Soc.*, 2016, 138(45), 14890–904.
44 P. A. Dub, B. L. Scott, J. C. Gordon. *J. Am. Chem. Soc.*, 2017, 139(3), 1245–60.
45 A. Anaby, M. Schelwies, J. Schwaben, F. Rominger, A. S. K. Hashmi, T. Schaub, *Organometallics*, 2018, 37(13), 2193–201.
46 D. J. Tindall, M. Menche, M. Schelwies, R. A. Paciello, A. Schäfer, P. Comba, et al., *Inorg. Chem.*, 2020, 59(7), 5099–115.
47 D. H. Nguyen, X. Trivelli, F. Capet, Y. Swesi, A. Favre-Réguillon, L. Vanoye, et al., *ACS Catal.*, 2018, 8(5), 4719–34.
48 (N. J. Oldenhuis, V. M. Dong, Z. Guan, *Tetrahedron*, 2014, 70(27), 4213–8.
49 T. Otsuka, A. Ishii, P. A. Dub, T. Ikariya, *J. Am. Chem. Soc.*, 2013, 135(26), 9600–3.
50 N. Bampos, L. D. Field, B. A. Messerle, *Organometallics*, 1993, 12(7), 2529–35.
51 Life Cycle Assessment Harmonization, https://www.nrel.gov/analysis/life-cycle-assessment.html, (accessed March 2024).
52 M. Nayal, A. Kr. Sharma, S. Jain, V. P. Singh, *Highly Efficient Thermal Renewable Energy Systems: Design, Optimization and Applications*, ed. V. Verma, M. Chitt, S. Thangavel, A. Kumar, Taylor & Francis Group, Boca Raton, 1, 2024, Chapter 11, p. 168–93.
53 H. Park, S. Yoon, *ACS Sustainable Chem. Eng.*, 2023, 11(32), 12036–44.
54 A. Monney, E. Barsch, P. Sponholz, H. Junge, R. Ludwig, M. Beller, *Chem. Commun.*, 2013, 50(6), 707–9.
55 M. Nielsen, E. Alberico, W. Baumann, H. J. Drexler, H. Junge, S. Gladiali, et al., *Nature*, 2013, 495(7439), 85–9.
56 R. E. Rodríguez-Lugo, M. Trincado, M. Vogt, F. Tewes, G. Santiso-Quinones, H. Grützmacher, *Nature Chem.*, 2013, 5(4), 342–7.
57 N. Onishi, G. Laurenczy, M. Beller, Y. Himeda, *Coordination Chemistry Reviews*, 2018, 373, 317–32.

Data availability

The data supporting this article has been included as part of Supplementary Information and CheckCIF files.